Tetrahedron Vol. 44, No. 8, pp. 2329 to 2338, 1988
Printed in Great Britain.

0040-4020/88 $3.00+.00

CONFORMATION OF A HEXAHYDROCANNABINOL DERIVATIVE VIA 1- AND 2-D NOE EXPERIMENTS. EVALUATION OF $^{1}J_{CH}$ COUPLING CONSTANTS BY SEMISELECTIVE 2-D J-SPECTROSCOPY AND THEIR CORRELATION WITH THE RING GEOMETRY

ANTONIO DE MARCO*, LUCIA ZETTA, ROBERTO CONSONNI and MASSIMO RAGAZZI

Istituto di Chimica delle Macromolecole del CNR
Via E. Bassini 15, 20133 Milano, Italy.

(*Received in UK* 5 *February* 1988)

ABSTRACT - The conformation of the hexahydrocannabinol derivative (-)-(6aR,9R,10aR)-6,6,9-trimethyl-6a,7,8,9,10,10a-hexahydro-6H-dibenzo[b,d]pyran (HHC) has been determined by 1- and 2-D NOE experiments, the latter obtained with a pulse sequence which strongly reduces the contribution of the main diagonal.

$^{1}J_{CH}$ and $^{3}J_{CH}$ have been measured in heteronuclear J-resolved 2-D spectra obtained both with the gated decoupling technique, and with "spin-flip" of directly attached protons ("semiselective" 2-D J-spectroscopy).

On the basis of the NOE effects, it can be concluded that the conformation of the pyran ring is essentially half-chair. This result is consistent with the $^{3}J_{CH}$'s measured between the geminal methyl carbons at C-6 and H-6a; at least one of the two couplings appears to be sensibly lowered by the nearby oxygen.

The $^{1}J_{CH}$'s appear to be directly related to the proton geometry, e.g. they are 127.7 Hz for the three equatorial protons at sites 7, 8 and 10 (see Fig. 1), and range between 123.4 and 124.8 Hz for the corresponding axial protons.

The attempt of determining structure and conformation of small molecules by NMR is hampered by a number of difficulties, mainly because highly crowded spectra with many overlapping resonances often remain unresolved, even at high magnetic fields.

Significant improvements of resolution can be achieved by spreading the spectra in a second dimension. Yet, conventional COSY[1] or DQF-COSY[2], etc, have not enough resolving power when the signal degeneracy is too severe. The resolution achieved by introducing an isotope other than proton in the second dimension has proved to be quite useful, especially when good sensitivity and digital resolution are still possible, as it is the case for hetero-correlated ^{13}C-^{1}H spectra obtained *via* proton detection and polarization transfer[3,4].

However, also in homonuclear 2-D experiments a number of pulse sequences have been proposed in recent years, which improve the spectral appearence and the resolution that can be achieved, particularly for coupled resonances close to each other, whose cross-peaks are easily obscured by the main diagonal.

Proton-carbon coupling constants are sensitive to structure and conformation. The vicinal $^{3}J_{CH}$ exhibits the usual angular dependence[5-9], although the effect of substituents is not completely clarified to date, which often prevents a clear interpretation of the data.

$^{1}J_{CH}$ is highly influenced by the hybridization of the carbon and by the stereochemistry of the coupled proton. In particular, in alicyclic compounds the heteronuclear coupling constants has been found to be slightly different for axial and equatorial protons[10].

$^{1}J_{CH}$ and $^{3}J_{CH}$ can be measured by 1- and 2-D NMR experiments, e.g. INEPT or DEPT spectra without proton decoupling during acquisition[11,12], heteronuclear J-resolved 2-D spectra obtained either with the gated decoupling technique, or with the so-called "spin-flip" method[13].

While any of the first three experiments proves to be suitable for evaluating the long-range ^{13}C-^{1}H coupling constants and the heteronuclear interactions across one bond for CH and CH_3 groups, the last one appears to be unique in order to measure the $^{1}J_{CH}$ in methylene groups. In fact, second order effects complicate the appearance of CH_2 multiplets in undecoupled ^{13}C spectra to the extent to prevent any significant evaluation of the heteronuclear interactions. A variation of the "spin-flip" method first introduced by Bax in 1983[14] and then reproposed by Rutar in 1984 with minor modifications[15] (semiselective 2-D J-spectroscopy) makes it possible to remove the long-range couplings from the spectrum, which causes great spectral simplification, disappearence of second order effects, and evidentiation of a possible difference between the two $^{1}J_{CH}$ in methylene groups.

An alternative way of separating the two $^{1}J_{CH}$'s is to look at the ^{13}C satellites of the ^{1}H signals, provided the geminal protons are separate enough in the spectrum. For complicate spectra this becomes completely unfeasible, but an elegant evolution of the experiment is to spread the satellites in a second dimension according to the carbon chemical shifts, by mean of the so-called reverse detection techniques[3,4].

Although cannabinoids have been the subject of clinical, pharmacological and chemical studies for many years, a fuller understanding of their activity requires more information than is presently available. It is generally recognized that a precise knowledge of the electronic and conformational features of a molecule can provide an insight into its biological mode of action.

In a previous paper, we discussed the structure and the stereochemistry of the hexahydrocannabinol derivative shown in Fig. 1 (HHC), mostly on the basis of carbon-carbon (2D-INADEQUATE) and proton-carbon connectivities obtained with proton detection[16].

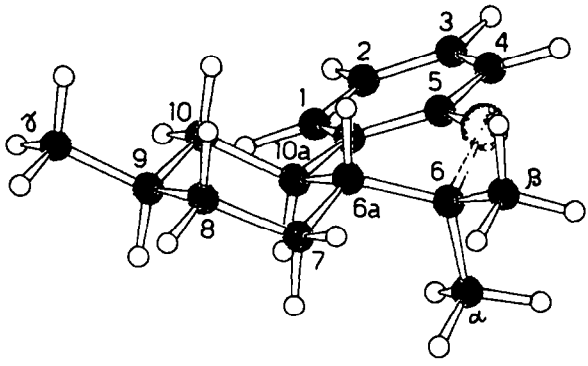

Fig. 1: Molecular model of HHC.

In the present communication we focus on the conformation of the pyran ring in HHC and on the orientation of the cyclohexane protons, presenting additional 2-D experiments, such as NOESY spectra obtained with a pulse sequence which strongly reduces the contribution of the main diagonal, hence the T_1 noise from the intense methyl peaks[17], and carbon-proton heteronuclear J-resolved spectra, with and without interactions across more than one bond[14-15].

While the values of the heteronuclear coupling constants appear to be related to the axial or equatorial geometry of the C-H bonds, the NOESY experiments suggest that the pyran ring is predominantly in the half-chair conformation.

The results are compared with those published by other authors on similar derivatives[18,19].

EXPERIMENTAL

The source of (-)-(6aR,9R,10aR)-6,6,9-trimethyl-6a,7,8,9,10,10a-hexahydro-6H-dibenzo[b,d]pyran (HHC) was described previously[20].

HHC solutions in C^2HCl_3 and $C_5{}^2H_5N$ were 20 and 5 mM, respectively. All NMR experiments were performed on a Bruker AM-270 spectrometer, equipped with an Aspect-3000 computer. Transient NOE experiments were performed by inverting the selected signal applying the decoupler frequency for 45 ms, with 40 dB attenuation, then allowing the system to evolve for 0.9 s before sampling.

The 2-D NOESY experiments were obtained with the procedure described by Denk et al.[17], based on the difference method first suggested by Bodenhausen and Ernst[21], in which two scans corresponding to the conventional NOESY are co-added, followed by subtraction of two transients which contain only the contribution from the diagonal peaks. Carrier frequency and sweep width were chosen to cover only the aliphatic region of the spectrum; 128 t_1 increments were implemented over 512 data points in t_2 dimension; mixing time was 0.6 s. Spectra were collected in the phase-sensitive mode, using the TPPI sequence. Fourier transform was performed after applying a line broadening of 4 Hz to the raw data in both dimensions, and zero-filling the data matrix to 1024x512.

Heteronuclear J-resolved spectra were recorded either with the gated-decoupling technique[22], or with spin-flip on directly attached protons[14-15]. As for the NOESY, only the aliphatic region was observed, implementing 256 t_1 increments on 4K data points with a sweep width of 2146 and 220 Hz in F_2 and F_1 dimensions, respectively. The data matrix was zero-filled to 1K in F_1 and a gaussian window was applied in both dimensions before Fourier transformation. J-resolved contour plot and sections are all presented in the phase-sensitive mode.

The spectral simulation shown in Fig. 8 was performed with the PANIC program (Bruker Aspect-3000 Software Package); a Gaussian lineshape was used, in order to account for the resolution enhancement routine applied to the experimental spectrum.

The models shown in Fig. 1 and Fig. 4 were obtained with the SCHAKAL program (by E. Keller) and with the STICK program (M.R.), respectively.

Molecular geometry and NOE calculations were performed with the REFINE program[23]. The geometry of conformer I (half-chair) was obtained by minimizing the conformational energy, starting from the X-ray coordinates[20], available for the analog substituted in positions 1 and 3 of the aromatic ring with one OH and one CH_3 group, respectively. To obtain the geometry of the half-boat conformation, approximate coordinates measured in a Dreiding model were introduced in the REFINE program and then adjusted until minimization was achieved.

The NOE's quoted in Table 1 were calculated for the two conformations according to Noggle and Schirmer[24], in a procedure essentially identical to that described by Brisson and Carver[25]. The isotropic rotational correlation time τ_c was varied until the calculated T_1 values[26,27] matched the experimental ones, measured by the inversion-recovery technique.

The final value was $\tau_c = 0.4 \times 10^{-10}$ s.

RESULTS AND DISCUSSION

1. NOE experiments and conformation of the pyran ring

The structural formula of HHC is shown in Fig. 1. The complete assignment of the ^1H NMR spectrum of HHC in C^2HCl_3 was reported in a preceeding paper[16].

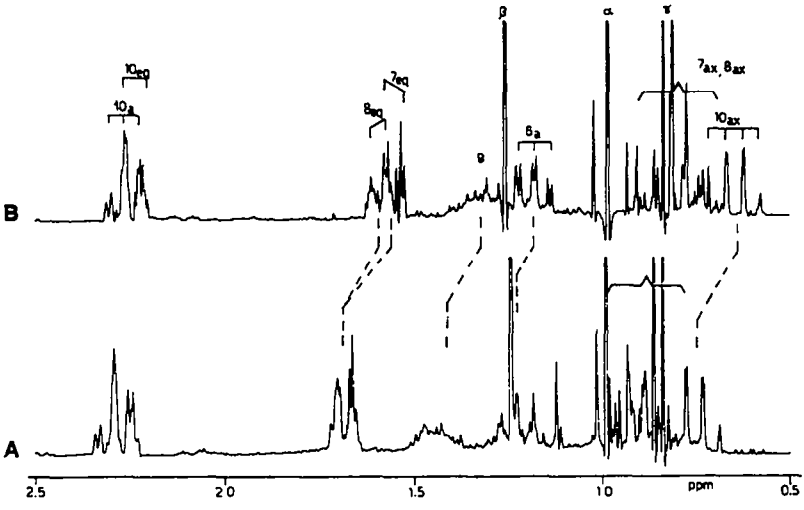

Fig. 2: ^1H NMR spectra of HHC at 270 MHz: aliphatic region in (A) C^2HCl_3, (B) $C_5{}^2H_5N$. Dotted lines connect shifted resonances between the two solvents.

Fig. 2 shows the aliphatic region of the ^1H NMR spectrum of HHC in solution of deuterated chloroform (A) and pyridine (B). As indicated by the dotted lines, a number of resonances exhibit shift variations from one solvent to the other, removing degeneracies which would make ambigous the interpretation of NOE effects in only one solvent. For example, the H-9 multiplet is neatly isolated in chloroform, whereas it partly overlaps with CH_3-β in pyridine, and the opposite occurs for H-6a, which resonates at the same frequency as CH_3-β in chloroform, but in pyridine is separate enough to distinguish its NOE effects from those of the methyl group.

Fig. 3 shows 1D transient NOE effects between aromatic and aliphatic protons, obtained for HHC in pyridine (see experimental section). Inversion of the aromatic proton H-1 causes a strong NOE

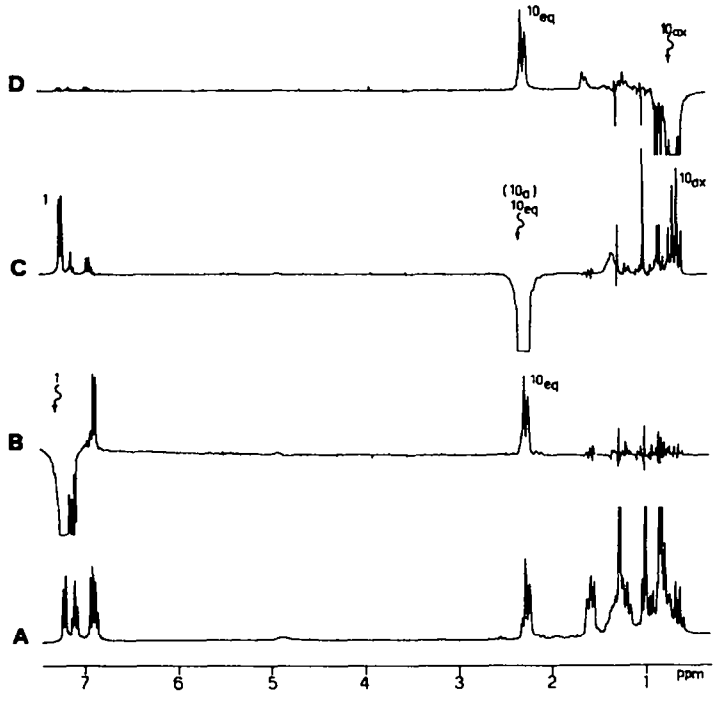

Fig. 3: 1-D transient NOE experiments on HHC in pyridine. (A), reference spectrum; (B), difference spectra following irradiation of protons indicated by the bent arrows. Positive NOE effects appear as positive peaks in the difference spectra.

to H-10_{eq} at the cyclohexane ring (B). Conversely, irradiation of H-10_{eq} perturbs H-1 and also its geminal H-10_{ax} (C). Finally, H-10_{ax} gives a strong NOE only to the geminal H-10_{eq} (D). No NOE is observed between H-1 and H-10_{ax}, by irradiating eitherone (B,D). By inspection of the molecular models (Fig. 4), it is seen that this is consistent with the half-chair conformation of the pyran ring, in which only H-10_{eq} is close to the aromatic proton H-1, while in the half-boat situation both H-10_{eq} and H-10_{ax} would be close enough to H-1 to give NOE.

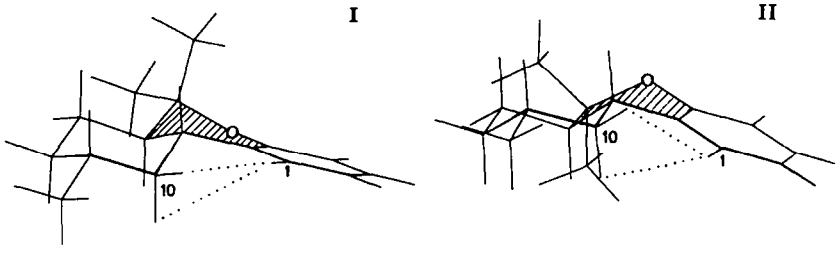

Fig. 4: Possible conformations for the pyran ring in HHC: half-chair (I) and half-boat (II).

The monodimensional experiment is satisfactory as long as the signals are well separate, but it lacks of selectivity in crowded spectral regions (such as that between 0.8 and 1.3 for HHC in both solvents, see Fig. 2), where neither the perturbed, nor the affected signals can often be established to a degree of reliability. A two-dimensional NOE experiment (NOESY) often provides the resolution required. However, the NOESY spectrum of HHC is particularly critical, as the methyl resonances are extremely intense when compared with the nearby multiplets (they have been cut-off in Figs. 2 and 3), and T_1 noise is so severe to prevent the detection of any significant cross peak in a wide spectral region (not shown). Fig. 5 shows two NOESY experiments on HHC in C^2HCl_3 (A) and $C_5{}^2H_5N$ (B), obtained with a pulse sequence proposed by Denk et al. in 1985[17], which eliminates most of the contribution of the main diagonal to the spectrum, hence reducing to a negligible extent the T_1 noise from intense peaks. The remainders of the main diagonal are however

of opposite sign when compared with the positive NOE's observed, and, as it can be seen in Fig. 5, in the "positive levels" representation only small wings are left, indicated by the dotted lines, representing the out-of-phase components of the spinning side bands.

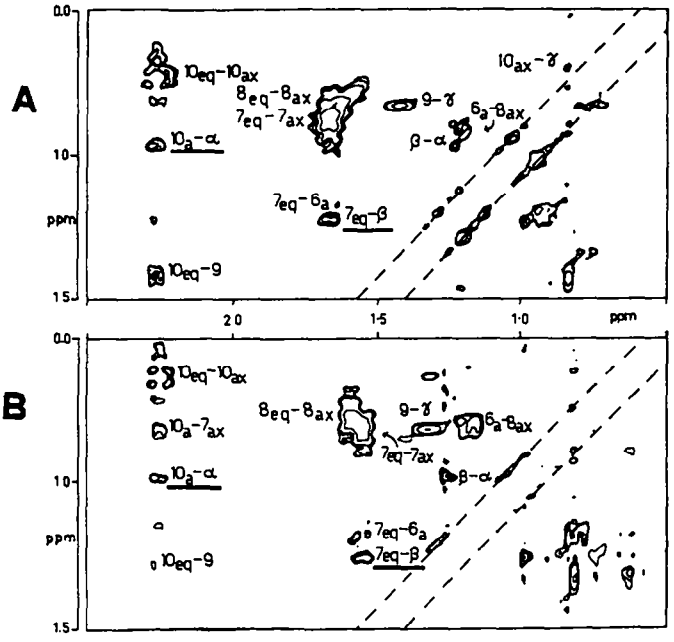

Fig. 5: 2D-NOESY experiments on HHC in (A) C^2HCl_3, (B) $C_5{}^2H_5N$, aliphatic region; contour plot of positive levels. The pulse sequence employed causes a strong reduction of the main diagonal contribution to the spectrum (see text). The most significant cross peaks are assigned in both spectra. The NOE's related to the conformation of the pyran ring are underlined. The two parallel dotted lines show residual spinning side bands of the main diagonal.

Although most of the NOE's in Fig. 5 are of structural origin, those between H-10a and CH_3-α and between H-7_{eq} and CH_3-β (underlined) are related to the conformation of the pyran ring. Moreover, such NOE's provide also the stereochemical assignment of the geminal methyl groups. NOE between H-10a and CH_3-α is possible only in the half-chair conformation, in which they are in <u>syn-periplanar</u> orientation, while H-7_{eq} would transmit NOE to the equatorial methyl, i.e. to CH_3-β in the half-chair and to CH_3-α in the half-boat conformation. Hence, the observation of a neat NOE effect between H-10a and one methyl group at C-6, both in chloroform and pyridine, sets for the half-chair conformation and assigns the higher field methyl singlet to the axial CH_3-α, and that at lower fields to the equatorial CH_3-β.

The NOE effect between one methyl singlet and H-10a was observed on a similar derivative by continous wave techniques[18], which already in 1970 suggested the predominance of the half-chair conformation.

Owing to the time-scale of the NMR experiments, the present results must be interpreted in a more flexible way, in that a small fraction of the half-boat form in rapid exchange with the predominant half-chair situation cannot be excluded. It could be objected to our conclusions that the presence of NOE's characteristic of the half-chair is not sufficient in order to assess that such conformation is the most populated, as NOE effects can be observed also for a relatively low conformer population. On the other hand, if the half-boat conformation would be present in a significant molar fraction, <u>its own</u> characteristic NOE's should appear in the spectra, such as that between H-10_{ax} and the aromatic proton H-1, which is not observed.

A more rigorous interpretation of the NOE data was made possible after calculation of the theoretical NOE's for the HHC molecule in the two conformations of the pyran ring. By using the well-known expression from Noggle and Schirmer[24], NOE effects were calculated from the molecular geometry, as described in the experimental section. Conversely, experimental NOE's were measured in 1- and 2-D spectra with standard area and volume integration, respectively. The results are compared in Table 1: it is unquestionable that only the half-chair conformation (I) is consistent

with the experimental NOE's: besides the already discussed NOE's between H-10a and CH_3-α and those between H-1 and HC-10_{eq} or H-10_{ax}, the presence of other intramolecular contacts, such as that between H-7_{eq} and CH_3-β, or the absence of dipolar interactions due only in the half-boat, like the one between H-7_{eq} and CH_3-α, reinforce the hypothesis of the predominance of the half-chair conformation.

Table 1. Comparison between experimental and theoretical NOE effects between protons in HHC. NOE's were calculated for two different conformations, according to Noggle and Schirmer[20] (see experimental section). Both experimental and calculated NOE's have been normalized to the highest value, i.e. to that between geminal protons at C-7 and C-8, taken as 100. Only NOE effects related to the conformation of the pyran ring are reported in the table. Experimental values are averaged between 1- and 2-D spectra (see text).

proton pair		conf. (I) half-chair calculated	experimental	conf. (II) half-boat calculated
H-1	H-10_{eq}	56	56	41
H-1	H-10_{ax}	0	0	15
H-6a	CH_3-β	4	NO*	15
H-10a	CH_3-α	24	27	0
H-7_{eq}	CH_3-β	28	21	0
H-7_{eq}	CH_3-α	0	0	31
H-7_{ax}	CH_3-α	8	NO*	15
H-10_{ax}	H-1	0	0	36
H-10_{eq}	H-1	132	103	102

* While "0" means that no NOE was observed, "NO" indicates that no NOE could be observed for technical reasons, e.g. because the involved proton resonances were too close in the spectrum.

2. $^3J_{CH}$'s and conformation of the pyran ring

The predominance of the half-chair conformation of the pyran ring should manifest also in the values of the $^3J_{CH}$'s measured between the geminal methyl carbons at C-6 and H-6a. Fig. 6 shows a contour plot of a heteronuclear ^{13}C-^1H J-resolved spectrum obtained with the "gated-decoupling" technique[22]. The reference spectrum on top labels the carbon resonances. Fig. 7 contains the 2-D

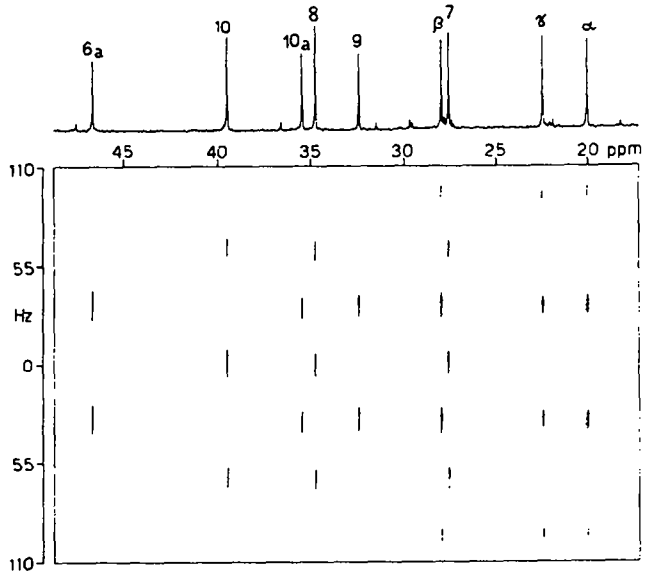

Fig. 6: ^{13}C-^1H Heteronuclear J-resolved spectrum of HHC obtained with the "gated-decoupling" technique, contour plot of the aliphatic region; the ^{13}C reference spectrum is shown above, with the resonance assignments.

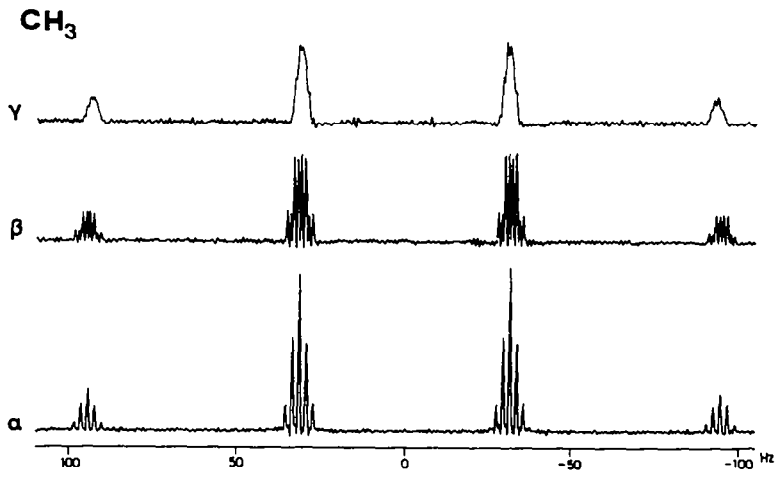

Fig. 7: Selected columns of the 2-D spectrum shown in Fig. 6, corresponding to the three methyl carbons α, β and γ.

matrix columns corresponding to the methyl resonances. The fine structure of the quartet components, due to heteronuclear coupling constants across more than one bond is neatly resolved for α and β methyls at C-6, whereas the γ methyl at C-9 presents scarcely resolved multiplets. In fact, the CH_3-α carbon is coupled to the CH_3-β protons across three bonds and viceversa, and the two methyl carbons are also coupled to H-6a via a $^3J_{CH}$. On the other hand, CH_3γ is coupled to H-9 across two bonds and to H-8_{ax}, H-8_{eq}, H-10_{ax} and H-10_{eq} across three bonds, which accounts for the broader appearence of the γ methyl resonances in Fig. 7.

The CH_3-α multiplets in Fig. 7 appear as a quintet of 4.2 Hz spacing, and the CH_3-β as a quartet of the same 4.2 Hz spacing, further doubled by a 2.5 Hz splitting. The interpretation is quite simple, as the 4.2 Hz coupling is from CH_3-α carbon to CH_3-β protons and viceversa, and the further splitting, i.e. again 4.2 Hz for CH_3-α and 2.5 Hz for CH_3-β carbons, is due to the $^3J_{CH}$ to H-6a. The latter coupling is directly related to the conformation of the pyran ring.

As most coupling constants across three bonds, also $^3J_{CH}$ depends on the dihedral angle between carbon and proton. Karplus-type equations obtained by INDO MO calculations on propane[7],

$$^3J_{CH} = 7.12 \cos^2 \theta - 1.00 \cos \theta + 0.70 \text{ Hz} \quad (1)$$

or by fitting experimental J values in systems of known geometry, such as the alumichrome peptide[8],

$$^3J_{CH} = 10.2 \cos^2 \theta - 1.3 \cos \theta + 0.2 \text{ Hz} \quad (2)$$

both lead to values of $^3J_{CH}$ for pure synclinal and antiperiplanar orientation of ≈ 2 Hz and ≥ 8 Hz, respectively.

The major problem in this approach is the effect of substituents on the coupling constants, which can be rather strong and is not easily quantified. As known by a number of studies on sugars and sugar derivatives, the values of the $^3J_{CH}$'s are strongly influenced by the presence of the oxygen in the ring; $^3J_{CH}$ values of 4-5 Hz were measured for anti and ≤ 2 Hz for gauche orientation in sugars[28,29]. This is consistent with the J values of 2.5 and 4.2 Hz measured for HHC, as in the half-chair conformation the methyl groups at C-6 are approximately in antiperiplanar and synclinal orientation with respect to H-6a.

Curves based on experimental points for uridine[5,6] and ^{13}C-labelled carbohydrates[9] have been also published, although in both cases the poor scattering of data did not allow to extract an analytical expression as those mentioned above, since e.g. the geometries corresponding to θ values ranging between 0 and 40 degrees were not represented by any experimental point.

Eventually, a further Karplus-type curve was proposed, based on ^{13}C NMR and X-Ray crystallographic data for a derivative of methyl β-cellobioside[30].

Table 2 lists the coupling constants from CH_3-α and CH_3-β carbons to H-6a, and to CH_3-α and CH_3-β protons, calculated using equations (1) and (2), or estimated from the curves of references[6,9,30], in which the θ angles correspond to the geometry of the half-chair (I) and of the half-

boat conformation (II).

Table 2. Heteronuclear $^3J_{CH}$ (Hz) of CH_3-α and CH_3-β in HHC: experimental, and calculated for the half-chair (I) and the half-boat conformation (II) using equations (1) and (2) or curves from references 6,9 and 30. The dihedral angles θ(deg) were calculated from the coordinates of the half-chair (I) and of the half-boat (II) conformers (see text).

I (half-chair)	θ(deg)	J(Hz)					
		exp	(1)	(2)	ref. 6	ref. 9	ref.30
Cα-C6-C6a-H6a	-165	4.25	8.33	11.00	6.3	4-5	5.5
Cβ-C6-C6a-H6a	74	2.50	0.96	0.60	0.5	1.5-2.5	0.8
Cα-C6-Cβ-H_3	*	4.25	4.26	5.30	≈3.5	3-5	≈3.5
Cβ-C6-Cα-H_3	*	4.25	4.26	5.30	≈3.5	3-5	≈3.5
II (half-boat)	θ(deg)	J(Hz)					
		exp	(1)	(2)	ref. 6	ref. 9	ref.30
Cα-C6-C6a-H6a	131	4.25	4.43	5.45	3	≈1	2
Cβ-C6-C6a-H6a	13	2.50	6.47	8.60	>4	>4	5
Cα-C6-Cβ-H_3	*	4.25	4.26	5.30	≈3.5	3-5	≈3.5
Cβ-C6-Cα-H_3	*	4.25	4.26	5.30	≈3.5	3-5	≈3.5

* averaged by free rotation.

As expected, owing to the presence of the oxygen in the pyran ring, the values obtained from (1) and (2) are higher than those experimentally observed, and no half-boat/half-chair ratio can account for the experimental couplings. Interestingly, we notice that the carbon-proton couplings measured between α and β methyls are identical to those predicted by eq. (1); this is probably due to the fact that for such interaction the oxygen is completely off the coupling path.

The $^3J_{CH}$ values calculated from references 6, 9 and 30 for the half-chair are in much better agreement with the experimental values, especially those extracted from the curve of Schwarcz and Perlin[9]. Unfortunately, if we reverse the assignment of α and β methyls in Table 2, the calculated J-values for the half-boat conformation are also in satisfactory agreement with the experimental values. Since the assignment of the methyl carbons is achieved *via* proton NOE and heteronuclear correlated spectra[16], we conclude that the $^3J_{CH}$'s measured between the methyl carbons at C-6 and H-6a are not *per se* sufficient to establish the conformation of the pyran ring.

3. $^1J_{CH}$'s and proton orientation

Fig. 8-I shows the 2-D matrix columns extracted from the contour plot of Fig. 6, corresponding to methylene carbons C-7, C-8 and C-10. Despite the resolution enhancement applied to the spectrum, extensive coupling prevents from extracting any significant information relative to the J_{CH} across more than one bond. As to the $^1J_{CH}$'s, an accurate detection is made difficult by (i) the resonance spread due to long-range couplings and (ii) second order effects transmitted to the carbons from strongly coupled protons. This latter phenomenon is particularly evident for C-7, whose resonance pattern is highly asymmetrical, and could be checked by simulating the proton-coupled carbon spectrum (see experimental section) as an eight spin system, containing ^{13}C-7 and all protons coupled across one (H-7_{ax} and H-7_{eq}), two (H-8_{ax}, H-8_{eq} and H-6a) and three bonds (H-9 and H-10a), with their relative chemical shifts and coupling constants. Starting values of the $^1J_{CH}$'s were obtained from our previous work[16]; the J_{CH}'s across more than one bond were slightly varied until the matching between experimental and calculated was satisfactory. The simulated spectrum of C-7 is shown in the top trace of Fig. 8-I.

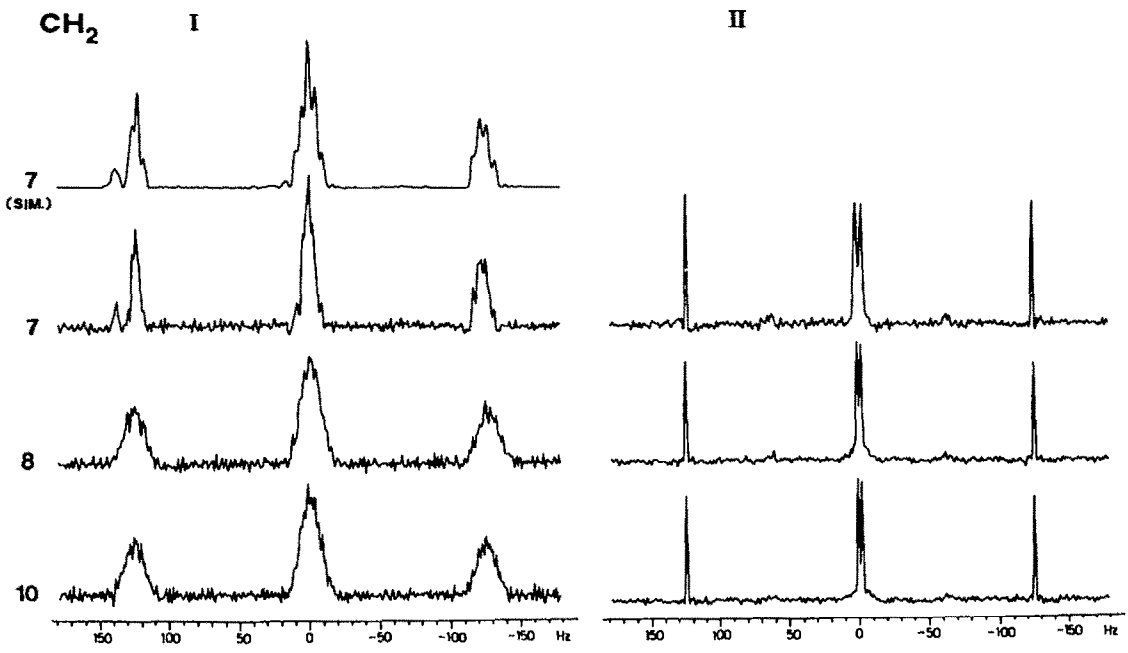

Fig. 8: (I), selected columns of the 2-D spectrum shown in Fig. 6, corresponding to the three methylene carbons C-7, C-8 and C-10; (II), same, but obtained with the "spin-flip" technique on directly attached protons. The top trace in (I) is the computer simulation of C-7 (see text).

It is clear from Fig. 8-I that a possible, small difference between the two $^1J_{CH}$'s in CH_2 groups is not likely to be detected in high resolution, proton-coupled carbon spectra, such as the heteronuclear J-resolved 2-D spectra obtained with the gated decoupling technique. In a recent communication on a cannabinol derivative similar to the one which is the subject of the present paper, by performing selective CW heteronuclear decoupling experiments, the authors detected a difference of 9 Hz between $^1J(C\text{-}10\text{--}H\text{-}10_{ax})$ and $^1J(C\text{-}10\text{--}H\text{-}10_{eq})$, while the corresponding coupling constants for C-7 and C-8 could not be distinguished[19], probably because the chemical shift between the geminal protons in both cases was too small.

We find that nowadays the so-called "semiselective J-resolved spectroscopy"[14,15], based on spin-flip methods, proves to be quite convenient for precise measurements of $^1J_{CH}$ in CH_2 groups, as it provides a way of selecting between one-bond and long-range heteronuclear interactions.

Fig. 8-II shows the same resonances as Fig. 8-I, in a J-resolved spectrum obtained with spin-flip on attached protons and consequent removal of carbon-proton couplings across more than one bond. The carbon resonances of the three methylene groups in positions 7, 8 and 10 are all neatly resolved into doublets of doublets. This indicates two distinct $^1J_{CH}$'s for each CH_2, hence, a definite dependence of the heteronuclear coupling constants on the proton orientation.

Table 3. Heteronuclear $^1J_{CH}$ (Hz) in HHC, as measured in J-resolved 2-D experiments with spin-flip on directly attached protons.

	C-6a	C-10	C-10a	C-8	C-9	C-7	C-α	C-β	C-γ
^1H (axial)	122.9	124.8	124.8	124.8	123.8	123.4			
^1H (equatorial)		127.6		127.6		127.6			
methyls							125.7	126.2	124.3

All $^1J_{CH}$'s for HHC are quoted in Table 3; the assignment of axial and equatorial interactions is from ref.[16]. As previously observed in cyclohexane[10], there is a definite correlation between

the magnitude of the coupling constants and the orientation of the involved protons, as the $^1J_{CH}$'s for equatorial protons are always bigger than those for axial protons. We detect a lower value for $^1J_{CHax}$ of C-7 (123.4 Hz) in comparison with those measured for C-8 and C-10 (124.8 Hz). On the other hand, we do not find the big difference between $^1J_{CHax}$ and $^1J_{CHeq}$ of C-10 measured for the analog subject of the paper by Hoffermann et al.[19]. The high value of $^1J_{CHeq}$ of C-10 (133 Hz) in that derivative could be ascribed to the fact that the benzene ring is replaced by the uracilic moiety.

Dr. Dino Ferro is gratefully acknowledged for helpful discussions concerning the calculations performed with the REFINE program[23].

1. A. Bax and R. Freeman, J.Magn.Reson. **42**, 164 (1981).

2. M. Rance, O.W. Sørensen, G. Bodenhausen, G. Wagner, R.R. Ernst and K. Wüthrich, Biochem.Biophys.Res.Commun. **117**, 479 (1983).

3. L. Müller, J. Am. Chem. Soc. **101**, 4481 (1979).

4. D. Brühwiler and G. Wagner, J.Magn.Reson. **69**, 546 (1986).

5. R.U. Lemieux, T.L. Nagabhushan and B. Paul, Can.J.Chem. **50**, 773 (1972).

6. L.T.J. Delbaere, M.N.G. James, and R.U. Lemieux, J.Am.Chem.Soc. **95**, 7866 (1973).

7. R. Wasylishen and T. Schäfer, Can.J.Chem. **50**, 961 (1973).

8. A. De Marco and M. Llinás, Biochemistry **18**, 3846 (1979).

9. J.A. Schwarcz and A.S. Perlin, Can.J.Chem. **50**, 3667 (1972).

10. V.A. Chertkov and N.M. Sergeyev, J.Amer.Chem.Soc. **99**, 6750 (1977).

11. G.A. Morris and R. Freeman, J.Am.Chem.Soc. **101**, 760 (1979).

12. D.M. Doddrell, D.T. Pegg and M.R. Bendall, J.Magn.Reson. **48**, 323 (1982).

13. G. Bodenhausen, R. Freeman, R. Niedermeyer and D.L. Turner, J.Magn.Res. **24**, 291 (1976).

14. A. Bax, J.Magn.Reson. **52**, 330 (1983).

15. V. Rutar, J.Magn.Reson. **56**, 87 (1984).

16. L. Zetta, A. De Marco, C. Anklin, M. Cornia and G. Casiraghi, Magn.Reson.Chem., in the press.

17. W. Denk, G. Wagner, M. Rance and K. Wüthrich, J.Magn.Reson. **62**, 350 (1985).

18. R.A. Archer, D.B. Boyd, P.V. Demarco, I.J. Tyminski and N.L. Allinger, J.Amer.Chem.Soc. **92**, 5200 (1970).

19. W. Offermann, W. Kuhn, J. Stelten, D. Leibfritz, G.v. Kiedrowski and L.F. Tietze, Tetrahedron **42**, 2215 (1986).

20. G. Casiraghi, M. Cornia, G. Casnati, G. Gasparri Fava and M. Ferrari Belicchi, J.Chem.Soc., Chem.Commun, 271 (1986).

21. G. Bodenhausen and R.R. Ernst, Mol.Phys. **47**, 319 (1982).

22. G. Bodenhausen, R. Freeman and D.L. Turner, J.Chem.Phys. **65**, 839 (1976).

23. M. Ragazzi and D.R. Ferro: "Model Building and Energy Minimization of Macromolecules Using the System REFINE with Univac Series 1100" Manual for Users, ICM, Milano, 1984.

24. J.H. Noggle and R.E. Schirmer (1971) The Nuclear Overhauser Effect, Academic Press, New York.

25. J.R. Brisson and J.P. Carver, Biochemistry **22**, 1362 (1983).

26. A. Kalk and H.J.C. Berendsen, J.Magn.Reson. **24**, 343 (1976).

27. B.D. Sykes, W.E. Hull and G.H. Snyder, Biophys.J. **21**, 137 (1978).

28. R.G.S. Ritchie, N. Cyr, and A.S. Perlin, Can.J.Chem. **54**, 2301 (1976).

29. K. Bock and C. Pedersen, Acta.Chem.Scand. **B31**, 354 (1977).

30. G.K. Hamer, F. Balza, N. Cyr and A.S. Perlin, Can.J.Chem. **56**, 3109 (1978).